



Original article

Trunk-to-leg volume and appendicular lean mass from a commercial 3-dimensional optical body scanner for disease risk identification

Jonathan P. Bennett^{a, *}, Michael C. Wong^a, Yong En Liu^a, Brandon K. Quon^a, Nisa N. Kelly^a, Andrea K. Garber^b, Steven B. Heymsfield^c, John A. Shepherd^a^a Department of Epidemiology, University of Hawai'i Cancer Center, 701 Ilalo St, Honolulu, HI, 96813, USA^b Division of Adolescent & Young Adult Medicine, University of California, San Francisco, 3333 California Street, Suite 245, San Francisco, CA, 94118, USA^c Pennington Biomedical Research Center, Louisiana State University, 6400 Perkins Rd, Baton Rouge, LA, 70808, USA

ARTICLE INFO

Article history:

Received 3 July 2024

Accepted 12 September 2024

Keywords:

3-dimensional optical
Trunk-to-leg volume
Appendicular lean mass
Metabolic syndrome
Body composition

SUMMARY

Background & aims: Body shape expressed as the trunk-to-leg volume ratio is associated with diabetes and mortality due to the associations between higher adiposity and lower lean mass with Metabolic Syndrome (MetS) risk. Reduced appendicular muscle mass is associated with malnutrition risk and age-related frailty, and is a risk factor for poor treatment outcomes related to MetS and other clinical conditions (e.g.; cancer). These measures are traditionally assessed by dual-energy X-ray absorptiometry (DXA), which can be difficult to access in clinical settings. The Shape Up! Adults trial (SUA) demonstrated the accuracy and precision of 3-dimensional optical imaging (3DO) for body composition as compared to DXA and other criterion measures. Here we assessed whether trunk-to-leg volume estimates derived from 3DO are associated with MetS risk in a similar way as when measured by DXA. We further explored if estimations of appendicular lean mass (ALM) could be made using 3DO to further improve the accessibility of measuring this important frailty and disease risk factor.

Methods: SUA recruited participants across sex, age (18–40, 40–60, >60 years), BMI (under, normal, overweight, obese), and race/ethnicity (non-Hispanic [NH] Black, NH White, Hispanic, Asian, Native Hawaiian/Pacific Islander) categories. Each participant had whole-body DXA and 3DO scans, and measures of cardiovascular health. The 3DO measures of trunk and leg volumes were calibrated to DXA to express equivalent trunk-to-leg volume ratios. We expressed each blood measure and overall MetS risk in quartile gradations of trunk-to-leg volume previously defined by National Health and Nutrition Examination Survey (NHANES). Finally, we utilized 3DO measures to estimate DXA ALM using ten-fold cross-validation of the entire dataset. **Results:** Participants were 502 (273 female) adults, mean age = 46.0 ± 16.5y, BMI = 27.6 ± 7.1 kg/m² and a mean DXA trunk-to-leg volume ratio of 1.47 ± 0.22 (females: 1.43 ± 0.23; males: 1.52 ± 0.20). After adjustments for age and sex, each standard deviation increase in trunk-to-leg volume by 3DO was associated with a 3.3 (95% odds ratio [OR] = 2.4–4.2) times greater risk of MetS, with individuals in the highest quartile of trunk-to-leg at 27.4 (95% CI: 9.0–53.1) times greater risk of MetS compared to the lowest quartile. Risks of elevated blood biomarkers as related to high 3DO trunk-to-leg volume ratios were similar to previously published comparisons using DXA trunk-to-leg volume ratios. Estimated ALM by 3DO was correlated to DXA ($r^2 = 0.96$, root mean square error = 1.5 kg) using ten-fold cross-validation.

Conclusion: Using thresholds of trunk-to-leg associated with MetS developed on a sample of US-representative adults, trunk-to-leg ratio by 3DO after adjustments for offsets showed significant associations to blood parameters and MetS risk. 3DO scans provide a precise and accurate estimation of ALM across the range of body sizes included in the study sample. The development of these additional measures improves the clinical utility of 3DO for the assessment of MetS risk as well as the identification of low muscle mass associated with poor cardiometabolic and functional health.

Published by Elsevier Ltd.

Abbreviations: 3DO, 3-dimensional optical; ADP, air displacement plethysmography; ALM, appendicular lean mass; AUC, area under the curve; BP, blood pressure; BG, blood glucose; BMI, body mass index; CVD, cardiovascular disease; DXA, dual energy X-ray absorptiometry; HDL, high-density lipoprotein; HOMA-IR, homeostatic model assessment for insulin resistance; MetS, Metabolic Syndrome; MRI, magnetic resonance imaging; TG, triglycerides.

* Corresponding author.

E-mail address: jbennett@cc.hawaii.edu (J.P. Bennett).

1. Introduction

As research between body composition measures and disease risk continues to grow, clinically accessible measures are increasingly valuable [2]. Earlier identification of over/undernutrition is critical to quantifying disease risk, preventing hospitalization, increasing awareness and education, and developing disease-mitigating interventions [3]. Systems capable of streamlining personal health status as well as provide measures associated with disease risk give healthcare providers opportunities to capture these measures as part of routine assessments.

Though less common during normal clinical screenings, dual-energy X-ray absorptiometry (DXA) systems are capable of whole-body and regional body composition measures linked to disease risk and outcomes. Wilson et al. (2013) showed that an increased trunk-to-leg volume, based on DXA scans in a representative sample of US adults, showed an increased risk of Metabolic Syndrome (MetS), cardiovascular disease (CVD), and mortality [4]. Their work showed that disease risk was driven by both increased fat mass and reduced muscle mass. Decreasing muscle mass across the lifespan is associated with impaired glucose tolerance, while decreased muscle strength due to muscle loss strongly relates to frailty and fall risk [5]. Given that an adult with normal weight could be at risk for both elevated truncal fat deposition and low muscle mass, routine clinical measures such as body mass index (BMI) and weight may not identify the increased disease risk resulting from elevated central obesity and decreased arm/leg muscle mass [6].

Alternatively, three-dimensional optical (3DO) systems have significant potential for use in monitoring disease risk factors due to their ease of use, rapidity of measures, and lack of ionizing radiation. These scans also provide a 3D avatar of body shape that has the potential to engage individuals in managing disease risks as opposed to monitoring numerical factors such as weight change [7–9]. Previously, we have shown the accuracy and precision of a clinical 3DO system of whole-body and regional measures of body composition and anthropometry compared to more costly or invasive laboratory measures (DXA and manual anthropometry) [1]. Further, we identified that body shape and composition features from 3DO measures improved the prediction of MetS risk as compared to demographic-based prediction models [10]. The purpose of this study was to determine if 3DO trunk-to-leg had a similar ability to identify those at risk of MetS and at-risk blood biomarkers as previously found in DXA studies. Further, using a machine learning approach, we assessed the accuracy and precision of a 3DO-based prediction equation for appendicular lean mass (ALM) compared to DXA.

2. Methods

This analysis included participants with data collected as part of the Shape Up! Adults study (NIH R01 DK109008, [clinicaltrials.gov](https://clinicaltrials.gov/ct2/show/study/NCT03637855) ID NCT03637855). The Shape Up! Adults study represents a diverse sample of adults with stratifications by sex, age (18–40 y, 40–60 y, >60 y), self-reported ethnicity (non-Hispanic White, non-Hispanic Black, Hispanic, Asian, and native Hawaiian or Pacific Islander), body mass index (BMI in kg/m^2 ; <18, 18–25, 25–30, >30), and geographic location (San Francisco, CA; Baton Rouge, LA; or Honolulu, HI). Full details of the study recruitment and procedures are outlined in the prior publication [1]. However, in brief, the methods used to collect data are outlined.

Body shape scans by 3DO were obtained using the Styku S100 scanner (Styku LLC, Los Angeles, CA, software version 4.1) while participants wore form-fitting shorts, a sports bra for females, and a swim cap. These clothes were also worn for whole-body DXA scans

on a Hologic Discovery/A system (Hologic Inc., Marlborough, MA). DXA scans were analyzed at UHCC by a trained technologist using Hologic Apex version 5.6 with the National Health and Nutrition Examination Survey (NHANES) Body Composition Analysis calibration option disabled. DXA regional measures include ALM (including bone mineral) and appendicular lean soft tissue (ALST; excluding bone mineral).

Fasting blood samples used for analysis included fasting blood glucose (BG), triglycerides (TG), insulin, and high-density lipoprotein cholesterol (HDL-C), while systolic/diastolic blood pressure (sBP/dBP) were measured at rest. Manual anthropometric measurements of waist circumference were collected and sex-specific cut points (88 cm in females, 102 cm in males) were combined with measures of BG, TG, HDL-C, and sBP/dBP for MetS diagnosis, as defined previously [10]. MetS was defined using the 2005 National Cholesterol Education Program Adult Treatment Panel III guidelines as having ≥ 3 of the following: high waist circumference, elevated TG (≥ 150 mg/dL), elevated blood pressure (≥ 130 mm Hg systolic or ≥ 85 mm Hg diastolic), elevated BG (≥ 100 mg/dL), and/or reduced HDL-C (< 40 mg/dL in males, < 50 mg/dL in females) [11]. Homeostatic model assessment for insulin resistance (HOMA-IR) was calculated as fasting insulin ($\mu\text{g}/\text{ml}$) * fasting glucose (mmol/l)/22.5. HOMA-IR values ≥ 2.9 were classified as having insulin resistance.

Regional body volume by DXA is based on the body volume models previously developed by Wilson et al. (2013) using air displacement plethysmography (ADP) as the criterion approach for whole-body volume measures [12]. In their study, DXA measures of fat, lean, and bone mineral were used to estimate volume based on the derivation of inverse densities of each component (1.05, 0.88, and 4.85 kg/L , respectively) and a residual component (0.01L). Using the DXA scan software, cut points are placed to differentiate regions of the arms, legs, and trunk. DXA whole-body volume estimates have been validated to ADP across multiple studies, though the differences in cut lines (detailed below) limit the ability to validate regional body volumes by DXA to criterion approaches such as magnetic resonance imaging (MRI) [13,14].

Trunk-to-leg volume is defined as the trunk volume divided by the sum of left and right legs. As detailed in our prior publication, the definitions for trunk and leg regions differ between DXA and those automatically derived from the 3DO software [1]. An example of the regional differences is presented in Fig. 1. The 3DO trunk

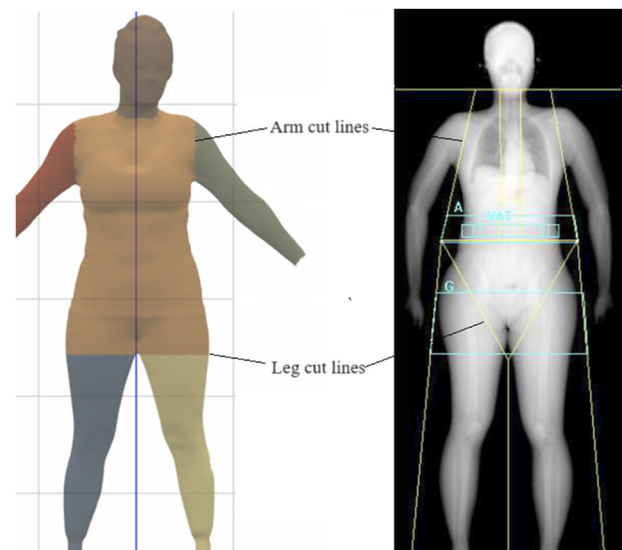


Fig. 1. Regional cut line differences between 3-dimensional optical (left) and dual-energy X-ray absorptiometry (right) systems.

volume (in liters) was therefore calibrated to DXA trunk volume using the previously published equation (3DO-calibrated Trunk Volume = $0.47 * 3DO \text{ Trunk Volume} + 10.16$). Leg 3DO volumes were found to have sex-specific associations to DXA: males (3DO-calibrated leg volume = $1.50 * 3DO \text{ leg volume} + 3.01$) and females (3DO-calibrated leg volume = $1.53 * 3DO \text{ leg volume} + 2.19$). Values for 3DO leg volume were performed using the regression equation for each leg, then summed to create leg volume. Finally, trunk-to-leg volume was calculated from these converted values ($3DO = \text{trunk volume} / [\text{right leg volume} + \text{left leg volume}]$). Data was divided into quartiles based on the DXA-derived trunk-to-leg volume from a representative sample of US adults in the NHANES as published in Wilson et al. (2013): Q1 (<1.34), Q2 (1.34–1.50), Q3 (1.50–1.65), and Q4 (>1.65) [4].

2.1. Statistical methods

For trunk-to-leg assessments, we determined the prevalence of MetS, HOMA-IR, and elevated blood markers in each quartile of trunk-to-leg volume by 3DO. We used logistic regression models to determine the association between trunk-to-leg and metabolic outcomes. For each model, we determined area under the curve (AUC) receiver operating characteristic, odds ratio per standard deviation (SD) increase of trunk-to-leg volume ratio, and odds ratios based on trunk-to-leg quartile (with Q1 as reference). Models were adjusted for age (Model 1) and age, sex, race/ethnicity, BMI, and waist circumference (Model 2). Model performance was compared to a non-linear approach, where restricted cubic splines were applied to the cutoffs of trunk-to-leg volume for both DXA and 3DO [15]. Logistic regression models were repeated using the pre-defined splines and the resulting AUCs were contrasted to the fully adjusted model (Model 2) [16].

To develop a 3DO ALM prediction model, a k-fold cross validation was performed to develop a prediction model while reducing the risk of overfitting. This machine learning approach divided the dataset into equal samples, where equations developed in each dataset were validated in the separate, unseen data [17]. Only measures available on the commercial version of the 3DO system were included. Measures that included right and left-sided values (e.g.; bicep or thigh circumference) were averaged and these average values were included as potential covariates in the prediction model. In each dataset, body composition, area, volume, and circumference (in centimeters) measures were entered using a SAS macro for kfold to divide the dataset into equal samples. Procedures included PROC GLMSELECT with stepwise selection and final variables remaining in the model if they were statistically significant ($p < 0.05$). Validation metrics were performed across k-folds ranging from 2 to 10 to ensure that the final fold size of 10 ($n = \sim 50$ participants/fold) was not too small to impact model performance. After reporting the assessment of each model to ensure robustness of the number of folds, the models were averaged into the final prediction model presented. Performance was evaluated using the coefficient of determination (r^2), root mean square error (RMSE), and Bland–Altman values to determine the mean difference (MD) and 95% limits of agreement (LoA). The estimate model was then repeated for ALST, excluding regional bone mineral, for use in low muscle mass assessment evaluations. Additionally, because two scans were performed using 3DO on each participant, test-retest precision was performed. Samples with only single measurements or non-physiologically plausible values were removed. Duplicate ALM values were calculated and the measurement precision was assessed using the coefficient of variation (CV) and RMSE assessments. Statistical analysis was performed using SAS version 9.4 for Windows (SAS Institute, Cary, NC).

3. Results

Of the 619 participants recruited, 502 participants had measures on both DXA and 3DO systems. Participant demographics and body composition measures are presented in Table 1. The distribution of participants into BMI categories or underweight (5.6%), normal weight (32.7%), overweight (33.3%), and obese (28.5%); a greater proportion of SUA participants were in the lower BMI categories compared to NHANES (underweight [1.7%], normal weight [33.0%], overweight [38.7%], and obese [26.6%]).

The mean \pm standard deviation for DXA trunk-to-leg volume in the SUA sample (1.47 ± 0.22) was similar to that reported in the NHANES sample (1.53 ± 0.24). Using the trunk-to-leg cut-offs previously derived using the NHANES dataset, the distribution of participants based on DXA (Q1 [$n = 136$, 27.1%], Q2 [$n = 161$, 32.1%], Q3 [$n = 100$, 19.9%], Q4 [$n = 105$, 20.9%]) was similar to 3DO (Q1 [$n = 130$, 25.9%], Q2 [$n = 160$, 31.9%], Q3 [$n = 107$, 21.3%], and Q4 [$n = 105$, 20.9%]). While participants in the SUA sample had a slightly lower proportion of individuals in the higher quartiles, they exhibited a higher rate of MetS (18.9%, $n = 95$) compared to NHANES (15.6%).

To compare the race/ethnic-specific average trunk-to-leg volume ratios, Supplement Table 1 provides the mean, standard deviation, minimum and maximum values, divided by sex. In females, the mean trunk-to-leg volume ratio for NH blacks (1.31 ± 0.21) was significantly lower (all $p < 0.05$) compared to all other groups. In males, NH Blacks were significantly lower than NH Whites ($p < 0.05$). However, the minimum and maximum values show that each race/ethnic group had individuals in all four trunk-to-leg volume ratios across both sexes.

The sex-specific prevalence of HOMA-IR and MetS based on trunk-to-leg quartiles are presented in Fig. 2. MetS prevalence increased from Q1 (2.2% in males, 6.3% in females) to Q4 (41.9% of males, 55.5% of females), with a significant ($p < 0.001$) trend of increasing prevalence with increasing trunk-to-leg quartile in both sexes. Similarly, across trunk-to-leg quartiles, the prevalence of elevated HOMA-IR increased significantly ($p < 0.001$) from Q1 (4.2% in males, 9.1% in females) to Q4 (71.2% in males, 53.3% in females).

Figure 3 presents the trends in individually measured blood parameters with increasing trunk-to-leg quartile. Each of the measured blood parameters showed a significant trend for increasing prevalence of impairment with increasing trunk-to-leg quartile, with elevated blood pressure having the greatest prevalence in Q4 (41.9% in males, 53.1% in females). While MetS prevalence was greater in females (Fig. 2), greater prevalence of elevated triglycerides was observed in Q4 males (36.6% versus 24.4% in females), while increased visceral adipose tissue area (105.1 cm^2 vs 93.2 cm^2 in females, $p < 0.05$; data not shown) was also observed.

Results of the area under the receiver–operator curves (AUC) for the estimation of cardiometabolic parameters based on trunk-to-leg as measured by DXA and 3DO calibration are presented in Table 2. AUCs for both approaches ranged from 0.706 to 0.804, with similar performance for DXA and 3DO-calibrated trunk-to-leg volumes. In the fully adjusted models, each SD increase in 3DO trunk-to-leg volume was associated with a significantly (all $p < 0.05$) increased risk for all cardiometabolic parameters, ranging from 1.4 (blood pressure and glucose) to 3.0 (MetS). Compared to Q1, a significantly greater risk for all cardiometabolic risk parameters was observed across Q3 and Q4 (except Q3 blood pressure). Using a non-linear approach with restricted cubic splines did not improve the model performance for MetS prediction by DXA (logistic AUC = 0.907, cubic spline AUC = 0.896) or 3DO (logistic AUC = 0.899, cubic spline AUC = 0.887), with similar results for each additional blood marker and HOMA-IR.

Table 1
Subject characteristics (n = 502).

Variable	Total			Females (n = 273)			Males (n = 229)		
	Mean (SD)	Min	Max	Mean (SD)	Min	Max	Mean (SD)	Min	Max
Age (years)	46.0 (16.5)	18.0	89.0	46.8 (16.4)	18.0	89.0	45.0 (16.5)	18.0	79.0
Height (cm)	168.1 (10.0)	144.1	202.1	161.8 (6.8)	144.1	181.0	175.6 (7.8) ^b	151.1	202.1
Weight (kg)	78.4 (22.3)	35.4	173.5	72.1 (21.4)	35.4	152.7	86.2 (21.0) ^b	40.6	173.5
BMI (kg/m ²)	27.6 (7.1)	14.2	52.3	27.5 (7.8)	14.2	51.9	27.9 (6.1)	16.5	52.3
DXA FFM (kg)	55.2 (15.0)	28.6	107.8	46.1 (9.7)	28.6	80.4	66.1 (12.9) ^b	34.0	107.8
DXA FM (kg)	23.2 (12.2)	5.0	72.7	25.9 (12.9)	6.3	72.7	20.1 (10.4) ^b	5.0	66.5
DXA FM (%)	28.8 (9.6)	9.0	53.3	34.2 (8.1)	12.6	53.3	22.3 (6.8) ^b	9.0	47.7
DXA TR/L Volume Ratio	1.47 (0.22)	0.88	2.46	1.43 (0.23)	0.88	2.21	1.52 (0.20) ^b	1.08	2.46
Waist circumference (cm)	93.3 (16.7)	59.4	157.1	91.7 (16.9)	60.5	157.1	95.2 (16.4) ^b	59.4	157.0

	Total		Females		Males	
	Count	%	Count	%	Count	%
Race/Ethnicity						
Asian	106	21.1	57	20.9	49	21.4
Hispanic	72	14.3	40	14.7	32	14.0
NH Black	131	26.1	69	25.3	62	27.1
NHOPI ^a	43	8.6	26	9.5	17	7.4
NH White	150	29.9	81	29.7	69	30.0
Age (years)						
18-39	196	39.0	101	37.0	95	41.5
40-59	165	32.9	91	33.3	74	32.3
≥60	141	28.1	81	29.7	60	26.2
BMI (kg/m²)						
<18.5	28	5.6	24	8.8	4	1.8
18.5-24.9	164	32.7	91	33.3	73	31.9
25.0-29.9	167	33.3	80	29.3	87	38.0
≥30.0	143	28.5	78	28.6	65	28.4
Insulin resistance						
Yes	154	30.7	79	30.5	75	32.8
No	348	69.3	194	69.5	154	67.2
Metabolic Syndrome						
Yes	95	18.8	55	20.1	40	17.5
No	410	81.2	218	79.9	189	82.5
3DO TR/L using NHANES DXA quartiles						
<1.34	130	25.9	86	31.5	44	19.2
1.34–1.50	160	31.9	87	31.9	73	31.9
1.50–1.65	107	21.3	51	18.7	56	24.5
≥1.65	105	20.9	49	17.9	56	24.5

Abbreviations: BMI: body mass index, DXA: dual energy X-ray absorptiometry, FFM: fat free mass, FM: fat mass, NH: non-Hispanic, SD: standard deviation, TR/L: trunk-to-leg ratio.

Percentage values are rounded.

^a NHOPI: native Hawaiian or Pacific Islander.

^b Values differ significantly (p < 0.05) between sexes.

For utilizing 3DO measures to estimate DXA ALM the results of each validation in the separate holdout samples of the folds (ranging from 2 to 10) were evaluated. There were no differences in RMSEs for 2-fold through 10-fold models (data not shown), therefore the 10-fold model was selected and evaluated for its performance. RMSEs for each of the ten folds ranged from 1.4 to 1.7 kg, with average mean differences of 0.0 kg and no mean biases observed. As a result, the averaging of models was used to generate the final prediction model to estimate ALM:

$$ALM_{3DO} = 2.11071 - 0.01743 * \text{age} + 1.19736 * \text{sex} + 0.18805 * \text{mass} + 0.04599 * \text{height} + 0.25842 * \text{lean mass} - 0.09186 * \text{hip circumference} + 0.03604 * \text{average mid-thigh circumference} + 0.03917 * \text{average lower bicep circumference} - 0.11593 * \text{lower waist circumference}.$$

Where sex = 1 for males and sex = 0 for females. Measurements for height and circumference are in cm, while mass and lean mass are in kg. The overall performance of the final model was $r^2 = 0.96$, RMSE = 1.5 kg, MD = 0.0 kg, and LoAs from -2.9–2.9 kg, as shown in Fig. 4. The results of the ALST (excluding bone mass) prediction were similar, $r^2 = 0.95$, RMSE = 1.5 kg, MD = 0.0 kg and LoAs from -3.0 to 3.0 kg, with this equation reported in Supplement Table 2 and the results presented in Supplement Fig. 1.

For precision estimates, 20 participants had only a single scan available. Additionally, n = 14 were removed due to having incorrect/improbable values for measurements included in the model (e.g.; thigh circumference = 0 cm). In the final sample that had complete duplicate 3DO measures (n = 468), precision estimates for duplicate 3DO ALM estimates were CV = 1.4%, RMSE = 0.34 kg.

4. Discussion

Using a large, diverse sample of adults, we showed that 3DO estimates of trunk-to-leg volume and ALM can be used to estimate cardiovascular disease risk. The implementation of these measures into commercial 3DO systems makes the assessment of MetS risk and/or estimation of low muscle mass more accessible to health-care providers. A tool such as 3DO allows for both cost-effective and frequent monitoring, particularly when implemented into smartphones [18]. The benefits of these approaches, in addition to other easily accessible health metrics, can increase opportunities for an individual to monitor their health [19]. These features, in addition visual representations of body shape, also serve as opportune measures for clinical education when developing diet and exercise recommendations.

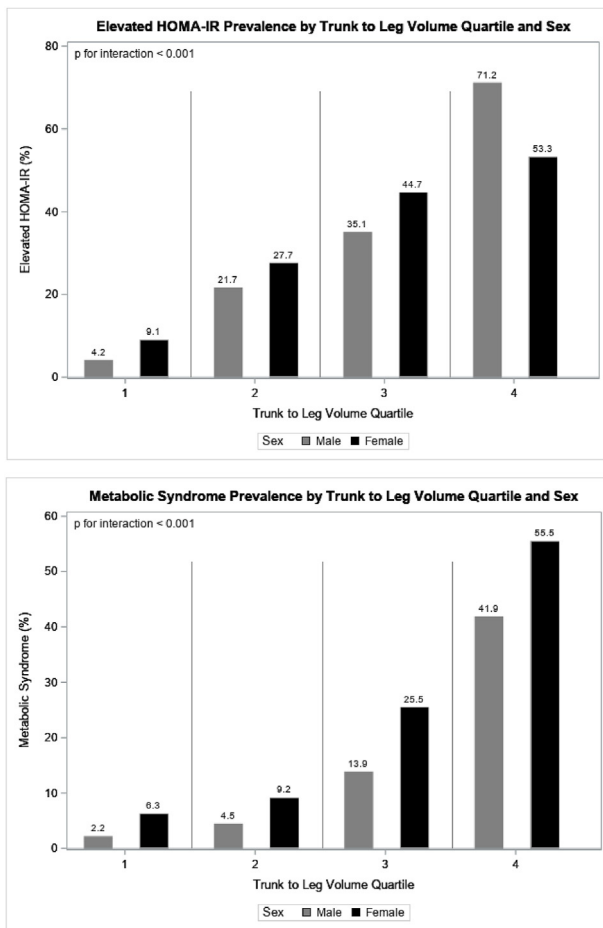


Fig. 2. Prevalence of insulin resistance (top) and Metabolic Syndrome (bottom) based on trunk-to-leg volume quartile using 3DO-calibrated estimates. Abbreviations: HOMA-IR, homeostatic model assessment for insulin resistance.

With rates of MetS risk increasing across the population, particularly with increasing prevalence being observed during younger adulthood, the quantification of disease risk poses a significant opportunity for earlier risk detection and intervention [20]. However, accessible clinical metrics such as body mass index fail to capture the changes in muscle and fat distribution that are associated with cardiometabolic disease risk across the lifespan [21]. Though anthropometry provides estimates of the distribution of muscle, fat, and visceral fat, significant limitations exist in terms of practicality and accuracy, particularly with monitoring changes with weight stability or age-related change [22]. With increased access to body composition assessment, novel indices provide opportunities to improve detection and risk monitoring.

As larger samples of body composition data are collected, measures of regional muscle and fat are showing closer associations with cardiovascular disease risk compared to whole-body measures [23]. DXA systems have been well documented for their ability to quantify disease risk based on regional fat and muscle distribution [21,24,25]. The derivation of body volume measures and the trunk-to-leg volume using DXA by Wilson et al. [4,12] allowed for the identification of novel body shape markers associated with disease risk. The derivation of trunk-to-leg ratio in NHANES showed that the predictive accuracy of this ratio was driven by both muscle and fat composition. This has led to multiple studies in NHANES datasets showing the positive associations of trunk fat and negative associations of leg fat to blood pressure in

adults and adolescents [26,27]. However, application of the trunk-to-leg volume ratio has not been assessed for its ability to identify disease risk in other populations. The results of this analysis show that the trunk-to-leg volume ratios derived from a nationally representative dataset successfully identified increased risk of cardiovascular disease parameters. The greater prevalence of elevated blood pressure (as well as other blood parameters) in the highest quartile of trunk-to-leg volume for DXA (data not shown) and 3DO support the findings regarding the impact of regional fat and muscle distribution on cardiovascular disease risk.

Our dataset showed that Q3 and Q4 of 3DO trunk-to-leg volume ratio were significantly associated with increased risk and overall prevalence of abnormal blood parameters as well as the presence of insulin resistance (as defined by HOMA-IR) and MetS. Interestingly, the prevalence of HOMA-IR in Q4 males (71.2%) was greater than females (53.3%). Females in Q4 showed greater prevalence of MetS (55.5% versus 41.9% in males) as well as each individual blood parameter with the exception of triglycerides. Previous studies have indicated that elevated triglycerides are associated with increased risk of insulin resistance [28]. Insulin resistance is a known precursor to cardiometabolic disease and the presence of high HOMA-IR in males may indicate increased likelihood of the progression of these males into MetS in the future, though the cross-sectional nature of this study prevents us from drawing these conclusions [29]. That said, the opportunity to monitor trunk-to-leg volume and changes in lean and fat masses through the use of 3DO provides the opportunity to monitor changes in body shape and composition that can support further insights into the factors that lead to MetS development [30].

In addition to regional fat and muscle distribution by trunk-to-leg volume ratio, low ALM has been linked to risk factors including diabetes, decreased bone density, and frailty/weakness [5,31,32]. Arm and leg muscles are most modifiable as a result of diet, physical activity, and aging, with increased musculature a protective factor against the development of diabetes and early mortality [33]. Muscle mass, particularly as measured by DXA, has been suggested to monitor risk across the lifespan and within patient populations [34–36]. However, these systems may be cost-prohibitive for clinical monitoring of dietary, physical activity, and chemoprevention interventions. Further, even though DXA is considered a low ionizing radiation imaging technique, it is reasonable to minimize radiation dose if alternatives are available. The findings of this study highlight how 3DO measures of trunk-to-leg volume, when calibrated to DXA, perform similarly in predicting the presence of individual cardiometabolic risk factors as well as overall MetS presence. These predictions are of similar accuracy to DXA in the same population, validating the previous model as well as showing the utility of the measure for risk assessment across diverse populations. Because trunk-to-leg volume ratio quartiles were derived from a nationally-represented sample of US adults and these ratios have a stronger association than fat alone, this metric provides clinically important tools for monitoring disease risk. Ultimately, the increased risk for those in Q3–Q4 were shown to have greater MetS prevalence, particularly in females. These models therefore provide an accurate screening model for MetS risk assessment, which agrees with previous work showing the importance of body shape as a predictor of MetS risk in adults across sex, age, and race/ethnicity [10,37].

The results also support that a prediction model based on body shape characteristics provides similar ALM estimates to other accessible techniques such as bioelectrical impedance analysis or smartphone-based 3DO [38,39]. The model included demographics as well as circumferences and lean mass measures, which clearly reflect body shape differences that improve the representation of variation in lean mass in the arms and legs across the adult lifespan.

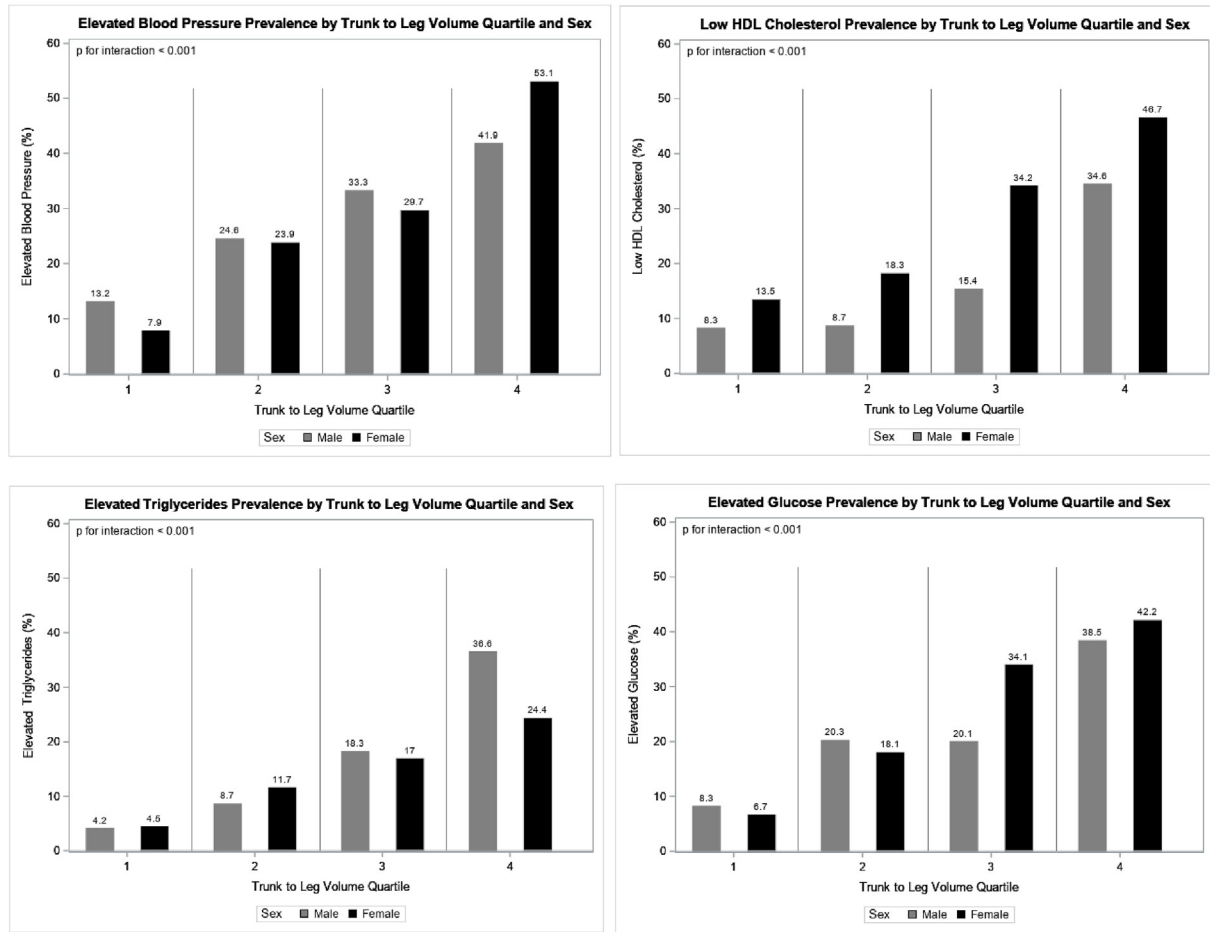


Fig. 3. Prevalence of impaired blood parameters based on trunk-to-leg volume quartile using 3DO-calibrated estimates.

Table 2

Logistic regression models to distinguish abnormal cardiovascular disease risk measures based on trunk-to-leg volume ratio.

DXA using NHANES quartiles							
Condition	Model	AUC	Per SD Increase	Q1 (n = 136)	Q2 (n = 161)	Q3 (n = 100)	Q4 (n = 105)
TG	Age	0.761	2.8 (2.1–3.8)	1	2.0 (0.7–5.8)	7.4 (2.6–20.8)	17.8 (6.3–50.2)
	Covariate	0.837	2.2 (1.5–3.1)		1.6 (0.5–5.1)	4.4 (1.4–14.0)	8.5 (2.7–27.3)
HDL-C	Age	0.680	2.0 (1.5–2.5)	1	1.2 (0.6–2.4)	2.8 (1.4–5.6)	5.7 (2.8–11.7)
	Covariate	0.779	1.8 (1.4–2.5)		1.4 (0.7–3.0)	2.9 (1.3–6.7)	5.0 (2.1–12.1)
BP	Age	0.713	1.3 (1.1–1.6)	1	0.8 (0.4–1.5)	1.1 (0.6–2.0)	2.0 (1.0–3.6)
	Covariate	0.753	1.2 (1.0–1.6)		0.7 (0.3–1.3)	0.8 (0.4–1.6)	1.3 (0.6–2.8)
BG	Age	0.782	2.0 (1.6–2.6)	1	1.5 (0.7–3.3)	3.0 (1.4–6.6)	6.1 (2.8–13.0)
	Covariate	0.820	1.9 (1.4–2.6)		1.4 (0.6–3.3)	2.7 (1.1–6.4)	5.1 (2.1–12.4)
HOMA-IR	Age	0.738	2.7 (2.1–3.5)	1	2.3 (1.2–4.5)	5.9 (3.0–11.6)	14.4 (7.1–29.3)
	Covariate	0.856	2.4 (1.7–3.3)		2.6 (1.2–5.8)	5.7 (2.3–13.9)	11.6 (4.5–30.1)
MetS	Age	0.790	3.4 (2.4–4.6)	1	0.9 (0.3–2.4)	3.5 (1.4–8.6)	13.0 (5.5–30.6)
	Covariate	0.907	2.6 (1.8–3.8)		0.7 (0.2–2.1)	2.0 (1.0–6.0)	6.2 (2.1–18.0)
3DO TR/L output by regression to DXA TR/L from [1] and using NHANES-derived quartiles							
Condition	Model	AUC	Per SD Increase	Q1 (n = 130)	Q2 (n = 160)	Q3 (n = 107)	Q4 (n = 105)
TG	Age	0.703	2.1 (1.6–2.8)	1	2.5 (1.0–6.7)	5.7 (2.1–14.9)	10.1 (3.8–26.8)
	Covariate	0.813	1.5 (1.0–2.1)		1.4 (0.5–3.7)	2.2 (1.2–6.0)	3.8 (1.7–10.9)
HDL-C	Age	0.729	2.0 (1.6–2.7)	1	2.4 (1.2–4.9)	4.0 (1.8–8.9)	7.9 (4.7–13.0)
	Covariate	0.781	1.6 (1.1–2.2)		1.9 (0.9–4.1)	2.7 (1.2–6.5)	6.5 (2.4–17.2)
BP	Age	0.718	1.5 (1.2–1.8)	1	1.1 (0.4–2.9)	1.7 (0.7–4.1)	2.6 (1.3–5.1)
	Covariate	0.754	1.4 (1.0–1.6)		1.0 (0.5–2.0)	1.5 (0.6–3.8)	2.5 (1.0–6.1)
BG	Age	0.757	1.8 (1.4–2.3)	1	2.7 (1.2–6.3)	4.4 (1.9–10.3)	6.8 (2.9–16.3)
	Covariate	0.808	1.4 (1.0–1.9)		1.8 (0.7–4.4)	2.5 (1.0–6.5)	3.1 (1.5–8.7)
HOMA-IR	Age	0.756	2.9 (2.2–3.8)	1	3.4 (2.5–5.8)	8.3 (4.2–13.4)	18.4 (12.4–32.8)
	Covariate	0.845	2.0 (1.4–2.4)		3.6 (1.5–9.2)	5.0 (2.4–13.2)	6.8 (3.0–19.7)
MetS	Age	0.797	3.2 (1.8–4.2)	1	1.0 (0.1–2.2)	3.8 (3.0–4.6)	8.0 (5.4–10.1)
	Covariate	0.899	3.0 (2.4–3.6)		0.9 (0.1–1.9)	3.5 (3.0–4.2)	7.1 (5.9–9.8)

Model 1 was adjusted for age, model 2 was adjusted for age, sex, race/ethnicity, BMI, and waist circumference.

Abbreviations: 3DO: 3-dimensional optical, AUC: area under the curve, BG: blood glucose, BP: blood pressure, DXA: dual energy X-ray absorptiometry, HDL-C: high-density lipoprotein cholesterol, HOMA-IR: homeostatic model assessment for insulin resistance, MetS: Metabolic Syndrome, TG: triglycerides.

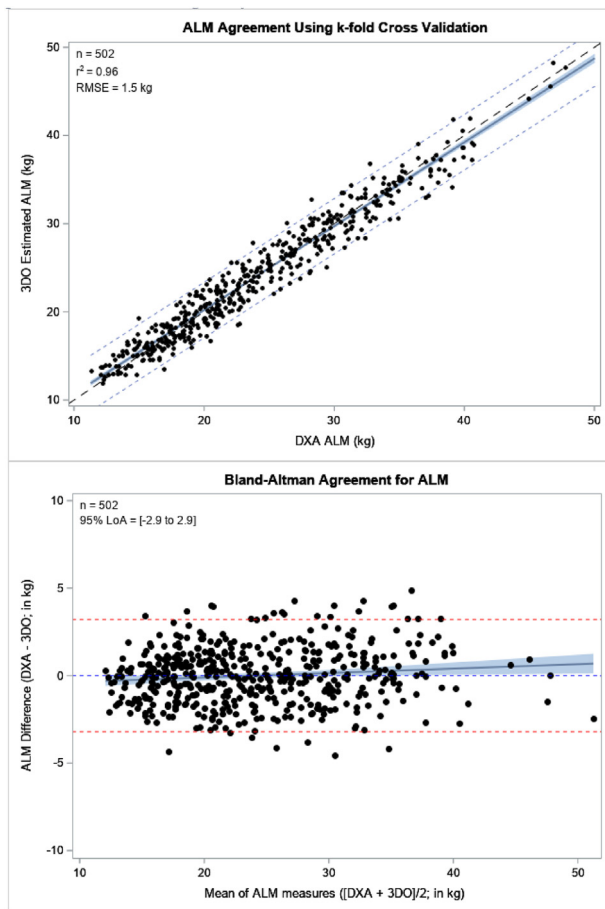


Fig. 4. Linear regression and Bland-Altman plots for final ALM prediction model using two-fold cross validation. Abbreviations: 3DO: 3-dimensional optical, ALM: appendicular lean mass, LoA: limits of agreement.

The precision estimates for duplicate measures were similar to those for fat-free mass from this and other 3DO scanners [1,40,41]. These results support the opportunity to use ALM estimates from 3DO to monitor regional muscle composition across the lifespan.

Advantages of this study include the large, diverse sample of adults as well as the significant proportion of the population with MetS. A limitation is that the cut points used by DXA systems (as well as limitations in criterion methods such as MRI, which often do not measure areas such as the head, feet, or hands) limit the opportunity to validate the regional volumes by DXA. That said, the DXA-volume approach applies physical modeling of pixel densities as well as empirical density estimates that reflect known physiological values [12,14]. Given that whole-body volume estimates have been validated to ADP, it is likely that this approach is accurate for regional estimates [13]. Clinically, the validity of this approach is supported by the strong prediction of MetS risk using both DXA and 3DO trunk-to-leg models, though we did not have data available to assess the links to other health outcomes, as performed previously [4]. It is also likely that the ALM prediction model may be limited due to the sample used to derive the equation, supporting the development of future models with improved performance. That said, we have shown the strong accuracy and precision of this model, while performing a machine learning cross-validation approach to avoid model overfitting. Finally, because these 3DO measures are device-specific, these results may differ from other 3DO systems that may utilize different regional volume cut lines.

In conclusion, 3DO offers a number of uniquely accessible features that make it an appealing tool for use in clinical practice as

well as across non-medical settings. We have shown that the additional features developed here can be implemented into these systems to further increase their utility for disease risk identification. These tools will aid healthcare professionals in capturing, quantifying, and educating the public regarding overall health and disease risk.

Funding

Funding for this study was part of the Shape Up! Adults grant (NIH R01 DK109008).

Disclosure

All authors report no conflict of interest.

CRediT authorship contribution statement

Jonathan P. Bennett: Conceptualization, Methodology, Formal analysis, Writing – original draft. **Michael C. Wong:** Resources, Methodology, Formal analysis, Writing – review & editing. **Yong En Liu:** Resources, Writing – review & editing, Investigation. **Brandon K. Quon:** Data curation. **Nisa N. Kelly:** Resources, Writing – review & editing, Project administration. **Andrea K. Garber:** Formal analysis, Writing – review & editing. **Steven B. Heymsfield:** Conceptualization, Writing – review & editing, Funding acquisition. **John A. Shepherd:** Conceptualization, Methodology, Writing – review & editing, Funding acquisition.

Conflict of interest

None.

Acknowledgements

We gratefully acknowledge the National Institutes of Health (NIH) for their funding and support of this research project. The authors would also like to thank the subjects for their participation in the Shape Up! Adults study.

Appendix A. Supplementary data

Supplementary data to this article can be found online at <https://doi.org/10.1016/j.clnu.2024.09.028>.

References

- [1] Bennett JP, Liu YE, Quon BK, Kelly NN, Wong MC, Kennedy SF, et al. Assessment of clinical measures of total and regional body composition from a commercial 3-dimensional optical body scanner. *Clin Nutr* 2022;41(1):211–8.
- [2] Thibault R, Genton L, Pichard C. Body composition: why, when and for who? *Clin Nutr* 2012;31(4):435–47.
- [3] Toomey CM, Cremona A, Hughes K, Norton C, Jakeman P. A review of body composition measurement in the assessment of health. *Top Clin Nutr* 2015;30(1):16–32.
- [4] Wilson JP, Kanaya AM, Fan B, Shepherd JA. Ratio of trunk to leg volume as a new body shape metric for diabetes and mortality. *PLoS One* 2013;8(7):e68716.
- [5] Cawthon PM, Peters KW, Shardell MD, McLean RR, Dam TTL, Kenny AM, et al. Cutpoints for low appendicular lean mass that identify older adults with clinically significant weakness. *The Journals of Gerontology Series A: Biological Sciences and Medical Sciences* 2014;69(5):567–75.
- [6] Shi TH, Wang B, Natarajan S. The influence of metabolic Syndrome in predicting mortality risk among US adults: importance of metabolic Syndrome even in adults with normal weight. *Prev Chronic Dis* 2020;17:E36.
- [7] Bennett J, Wong MC, McCarthy C, Fearnbach N, Queen K, Shepherd J, et al. Emergence of the adolescent obesity epidemic in the United States: five-decade visualization with humanoid avatars. *Int J Obes* 2022;46(9):1587–90.

- [8] Wong MC, McCarthy C, Fearnbach N, Yang S, Shepherd J, Heymsfield SB. Emergence of the obesity epidemic: 6-decade visualization with humanoid avatars. *Am J Clin Nutr* 2022;115(4):1189–93.
- [9] Minetto MA, Pietrobello A, Busso C, Bennett JP, Ferraris A, Shepherd JA, et al. Digital anthropometry for body circumference measurements: European phenotypic variations throughout the decades. *J Personalized Med* 2022;12(6):906.
- [10] Bennett JP, Liu YE, Quon BK, Kelly NN, Leong LT, Wong MC, et al. Three-dimensional optical body shape and features improve prediction of metabolic disease risk in a diverse sample of adults. *Obesity* 2022;30(8):1589–98.
- [11] Grundy SM, Cleeman JI, Daniels SR, Donato KA, Eckel RH, Franklin BA, et al. Diagnosis and management of the metabolic Syndrome. *Circulation* 2005;112(17):2735–52.
- [12] Wilson JP, Fan B, Shepherd JA. Total and regional body volumes derived from dual-energy X-ray absorptiometry output. *J Clin Densitom* 2013;16(3):368–73.
- [13] Ng BK, Liu YE, Wang W, Kelly TL, Wilson KE, Schoeller DA, et al. Validation of rapid 4-component body composition assessment with the use of dual-energy X-ray absorptiometry and bioelectrical impedance analysis. *Am J Clin Nutr* 2018;108(4):708–15.
- [14] Heymsfield SB, Smith B, Wong M, Bennett J, Ebbeling C, Wong JM, et al. Multicomponent density models for body composition: review of the dual energy X-ray absorptiometry volume approach. *Obes Rev* 2021:e13274.
- [15] Harrell FE. Regression modeling strategies. Springer Series in Statistics; 2001.
- [16] Nieboer D, Vergouwe Y, Roobol MJ, Ankerst DP, Kattan MW, Vickers AJ, et al. Nonlinear modeling was applied thoughtfully for risk prediction: the Prostate Biopsy Collaborative Group. *J Clin Epidemiol* 2015;68(4):426–34.
- [17] Beating the hold-out: bounds for k-fold and progressive cross-validation. In: Blum A, Kalai A, Langford J, editors. Proceedings of the twelfth annual conference on Computational learning theory; 1999.
- [18] Smith MK, Staynor JMD, El-Sallam A, Ebert JR, Ackland TR. Longitudinal concordance of body composition and anthropometric assessment by a novel smartphone application across a 12-week self-managed weight loss intervention. *Br J Nutr* 2023;1–7.
- [19] Bennett JP, Cataldi D, Liu YE, Kelly NN, Quon BK, Schoeller DA, et al. Development and validation of a rapid multicompartiment body composition model using 3-dimensional optical imaging and bioelectrical impedance analysis. *Clin Nutr* 2024;43:346–56.
- [20] Hirode G, Wong RJ. Trends in the prevalence of metabolic Syndrome in the United States, 2011–2016. *JAMA* 2020;323(24):2526.
- [21] Srikanthan P, Horwich TB, Tseng CH. Relation of muscle mass and fat mass to cardiovascular disease mortality. *Am J Cardiol* 2016;117(8):1355–60.
- [22] Gearon E, Tanamas SK, Stevenson C, Loh VH, Peeters A. Changes in waist circumference independent of weight: implications for population level monitoring of obesity. *Prev Med* 2018;111:378–83.
- [23] Okura T, Nakata Y, Yamabuki K, Tanaka K. Regional body composition changes exhibit opposing effects on coronary heart disease risk factors. *Arterioscler Thromb Vasc Biol* 2004;24(5):923–9.
- [24] Chen G-C, Arthur R, Iyengar NM, Kamensky V, Xue X, Wassertheil-Smoller S, et al. Association between regional body fat and cardiovascular disease risk among postmenopausal women with normal body mass index. *Eur Heart J* 2019;40(34):2849–55.
- [25] Zhou R, Chen HW, Lin Y, Li FR, Zhong Q, Huang YN, et al. Total and regional fat/muscle mass ratio and risks of incident cardiovascular disease and mortality. *J Am Heart Assoc* 2023;12(17):e030101.
- [26] Zhao S, Tang J, Zhao Y, Xu C, Xu Y, Yu S, et al. The impact of body composition and fat distribution on blood pressure in young and middle-aged adults. *Front Nutr* 2022;9:979042.
- [27] Cioffi CE, Alvarez JA, Welsh JA, Vos MB. Truncal-to-leg fat ratio and cardiometabolic disease risk factors in US adolescents: NHANES 2003–2006. *Pediatr Obes* 2019;14(7):e12509.
- [28] Ma M, Liu H, Yu J, He S, Li P, Ma C, et al. Triglyceride is independently correlated with insulin resistance and islet beta cell function: a study in population with different glucose and lipid metabolism states. *Lipids Health Dis* 2020;19(1).
- [29] Ormazabal V, Nair S, Elfeky O, Aguayo C, Salomon C, Zuñiga FA. Association between insulin resistance and the development of cardiovascular disease. *Cardiovasc Diabetol* 2018;17(1).
- [30] Wong MC, Bennett JP, Leong LT, Tian IY, Liu YE, Kelly NN, et al. Monitoring body composition change for intervention studies with advancing 3D optical imaging technology in comparison to dual-energy X-ray absorptiometry. *Am J Clin Nutr* 2023;117(4):802–13.
- [31] Li S, Mao J, Zhou W. Prediabetes is associated with loss of appendicular skeletal muscle mass and sarcopenia. *Front Nutr* 2023;10.
- [32] Ho-Pham LT, Nguyen UDT, Nguyen TV. Association between lean mass, fat mass, and bone mineral density: a meta-analysis. *J Clin Endocrinol Metabol* 2014;99(1):30–8.
- [33] Abramowitz MK, Hall CB, Amodu A, Sharma D, Androga L, Hawkins M. Muscle mass, BMI, and mortality among adults in the United States: a population-based cohort study. *PLoS One* 2018;13(4):e0194697.
- [34] Deutz NEP, Ashurst I, Ballesteros MD, Bear DE, Cruz-Jentoft AJ, Genton L, et al. The underappreciated role of low muscle mass in the management of malnutrition. *J Am Med Dir Assoc* 2019;20(1):22–7.
- [35] Chen Z, Wang Z, Lohman T, Heymsfield SB, Outwater E, Nicholas JS, et al. Dual-energy X-ray absorptiometry is a valid tool for assessing skeletal muscle mass in older women. *J Nutr* 2007;137(12):2775–80.
- [36] Garber AK, Bennett JP, Wong MC, Tian IY, Maskarinec G, Kennedy SF, et al. Cross-sectional assessment of body composition and detection of malnutrition risk in participants with low body mass index and eating disorders using 3D optical surface scans. *Am J Clin Nutr* 2023;118(4):812–21.
- [37] Lee JJ, Freeland-Graves JH, Pepper MR, Yu W, Xu B. Efficacy of thigh volume ratios assessed via stereovision body imaging as a predictor of visceral adipose tissue measured by magnetic resonance imaging. *Am J Hum Biol* 2015;27(4):445–57.
- [38] Bennett JP, Liu YE, Kelly NN, Quon BK, Wong MC, McCarthy C, et al. Next generation smartwatches to estimate whole body composition using bio-impedance analysis: accuracy and precision in a diverse multiethnic sample. *Am J Clin Nutr* 2022;116(5):1418–29.
- [39] McCarthy C, Tinsley GM, Yang S, Irving BA, Wong MC, Bennett JP, et al. Smartphone prediction of skeletal muscle mass: model development and validation in adults. *Am J Clin Nutr* 2023;117(4):794–801.
- [40] Ng BK, Sommer MJ, Wong MC, Pagano I, Nie Y, Fan B, et al. Detailed 3-dimensional body shape features predict body composition, blood metabolites, and functional strength: the Shape Up! studies. *Am J Clin Nutr* 2019;110(6):1316–26.
- [41] Wong MC, Bennett JP, Quon B, Leong LT, Tian IY, Liu YE, et al. Accuracy and precision of 3-dimensional optical imaging for body composition by age, BMI, and ethnicity. *Am J Clin Nutr* 2023;118(3):657–71.